Obesogenic diet in aging mice disrupts gut microbe composition and alters neutrophil:lymphocyte ratio, leading to inflamed milieu in acute heart failure

V. Kain, W. van Der Pol, N. Mariappan, A. Ahmad, P. Eipers, D. L. Gibson, Cécile Gladine, C. Vigor, Thierry Durand, C. Morrow, et al.

Obesogenic diet in aging mice disrupts gut microbe composition and alters neutrophil:lymphocyte ratio, leading to inflamed milieu in acute heart failure

Vasundhara Kain,[*] William Van Der Pol,[†] Nithya Mariappan,[‡] Aftab Ahmad,[‡] Peter Eipers,[§] Deanna L. Gibson,[¶] Cecile Gladine,[‖] Claire Vigor,[#] Thierry Durand,[#] Casey Morrow,[§] and Ganesh V. Halade[*,1]

[*]Division of Cardiovascular Disease, Department of Medicine, [†]Biomedical Informatics, Center for Clinical and Translational Sciences, [‡]Department of Anesthesiology and Perioperative Medicine, and [§]Department of Cell, Developmental, and Integrative Biology, The University of Alabama at Birmingham, Birmingham, Alabama, USA; [¶]Department of Biology, University of British Columbia Okanagan, Kelowna, British Columbia, Canada; [‖]Unité de Nutrition Humaine (UNH), Institut National de la Recherche Agronomique (INRA), Centre de Recherche en Nutrition Humaine (CRNH) Auvergne, Université Clermont Auvergne, Clermont-Ferrand, France; and [#]Unité Mixte de Recherche (UMR) 247, Institut des Biomolécules Max Mousseron (IBMM), Centre National de la Recherche Scientifique (CNRS), Ecole Nationale Supérieure de Chimie de Montpellier (ENSCM), University of Montpellier, Montpellier, France

ABSTRACT: Calorie-dense obesogenic diet (OBD) is a prime risk factor for cardiovascular disease in aging. However, increasing age coupled with changes in the diet can affect the interaction of intestinal microbiota influencing the immune system, which can lead to chronic inflammation. How age and calorie-enriched OBD interact with microbial flora and impact leukocyte profiling is currently under investigated. Here, we tested the interorgan hypothesis to determine whether OBD in young and aging mice alters the gut microbe composition and the splenic leukocyte profile in acute heart failure (HF). Young (2-mo-old) and aging (18-mo-old) mice were supplemented with standard diet (STD, ~4% safflower oil diet) and OBD (10% safflower oil) for 2 mo and then subjected to coronary artery ligation to induce myocardial infarction. Fecal samples were collected pre- and post–diet intervention, and the microbial flora were analyzed using 16S variable region 4 rRNA gene DNA sequencing and Quantitative Insights Into Microbial Ecology informatics. The STD and OBD in aging mice resulted in an expansion of the genus *Allobaculum* in the fecal microbiota. However, we found a pathologic change in the neutrophil:lymphocyte ratio in aging mice in comparison with their young counterparts. Thus, calorie-enriched OBD dysregulated splenic leukocytes by decreasing immune-responsive F4/80$^+$ and CD169$^+$ macrophages in aging mice. OBD programmed neutrophil swarming with an increase in isoprostanoid levels, with dysregulation of lipoxygenases, cytokines, and metabolite-sensing receptor expression. In summary, calorie-dense OBD in aging mice disrupted the composition of the gut microbiome, which correlates with the development of integrative and system-wide nonresolving inflammation in acute HF.—Kain, V., Van Der Pol, W., Mariappan, N., Ahmad, A., Eipers, P., Gibson, D. L., Gladine, C., Vigor, C., Durand, T., Morrow, C., Halade, G. V. Obesogenic diet in aging mice disrupts gut microbe composition and alters neutrophil:lymphocyte ratio, leading to inflamed milieu in acute heart failure. FASEB J. 33, 000–000 (2019). www.fasebj.org

KEY WORDS: inflammation · leukocytes · myocardial infarction · resolution of inflammation · nonresolving inflammation

Calorie-dense obesogenic diet (OBD) is the most controversial risk factor for obesity and obesity-related cardiovascular disease due to ischemic and nonischemic cardiac pathology (1). However, the inter-organ mechanism and disease pathology is incomplete, particularly in the age-related disease phase of life (*i.e.*, in aging). Furthermore,

ABBREVIATIONS: *Alox-5*, arachidonate 5-LOX; *Alox-12*, arachidonate 12-lipoxygenase; *Arg-1*, arginase 1; *Ccl2*, C-C motif chemokine ligand 2; *FPR*, formyl peptide receptor; *GPR*, G-protein coupled receptor; HF, heart failure; LOX, lipoxygenase; LV, left ventricle; Ly6C, lymphocyte antigen 6 complex, locus C; Ly6C^{hi}, high Ly6C; Ly6C^{lo}, low Ly6C; Ly6G, lymphocyte antigen 6 complex locus G; MI, myocardial infarction; MRC-1, mannose receptor C-type 1; MS/MS, tandem MS; MZ, marginal zone; OBD, obesogenic diet; OTU, operational taxonomic unit; PCoA, principal coordinates analysis; QIIME, Quantitative Insights Into Microbial Ecology; RP, red pulp; STD, standard diet; WP, white pulp; *Ym-1*, chitinase-like protein 3

[1] Correspondence: Division of Cardiovascular Disease, Department of Medicine, The University of Alabama at Birmingham, 310A Zeigler Research Building, 703 19th St. South, Birmingham, AL 35294, USA. E-mail: ganeshhalade@uabmc.edu

the prevalence of chronic heart failure (HF) increases with age, in part because of increased incidences of obesity, insulin resistance, and diabetes (2). Our previous study suggests that OBD intensified the post-myocardial acute inflammatory response in aging with the marked sign of nonresolving inflammation in heart and renal organs (3). An imbalance of nutrients and diet, exercise, and sleep are the ultimate cause of many cardiometabolic diseases (4). From a nutrition and obesity epidemic perspective, the American diet is enriched with n-6 fatty acids (*e.g.*, linoleic acid), and the percentage of n-6 fatty acids has increased from 3 to 7.21% (which is quite similar to the trend noted in the Australian population) because of industrialization and labor-saving technology (4–6).

Age-dependent diet and nutrient interaction with host intestinal microbiota plays a fundamental role in the function and defense training of the immune system (7). The commensal microbiota promotes and calibrates multiple aspects of the immune defense system, in contrast, the imbalance of intestinal microbiota or microbiome, a phenomenon termed dysbiosis that leads to several chronic inflammatory diseases including obesity, insulin resistance, and diabetes (8). However, age-related diversification of nutrients-microbial flora interaction is unclear. The diet-responsive and age-dependent microbiome consists of an integrative system of micro-organisms, which covers over a million different species of commensal bacteria, including a small amount of potentially pathogenic bacteria surviving in a symbiotic relationship with its host (9). Evolutionary, both humans and mice have relatively similar immune systems, microbiota, and susceptibility to encounter infectious agents and respective diseases (10–12). Two major bacterial phyla are present in the in the human gut, Bacteroidetes and Firmicutes, and a smaller number of bacteria are represented by the proteobacteria and actinobacteria phyla (9, 13). The Bacteroidetes and Firmicutes phyla are of major interest as both mouse and human shared many classes and families of these phyla (10). An alteration in the ratio of these phyla in response to diet or age is also known to occur in inflammatory bowel disease, aging, diabetes, and the metabolic syndrome (14). High levels of n-6 with low levels of-n-3 fatty acids in the diet has been linked to several other proinflammatory conditions such as insulin resistance, atherosclerosis, diabetes, and myocardial infarction (MI) (15–19). Disruption of immune-responsive bacterial populations due to aging and diet alteration on the immunologic scale is incomplete. Therefore, the current study was designed to define the interorgan interaction of n-6 fatty acids enriched diet with microbiome and the splenic immune response in aging during acute HF.

Age-associated dysbiosis is marked by the change in the ratio of the major bacterial phyla in the gut (20). Furthermore, age-related derangement of human and mice have been shown in the Firmicutes population, and a higher abundance of facultative anaerobic bacteria is associated with increased inflammation (21). It has also been shown that diet independently dysregulates microbiome (8, 22) but it is not known if how age-related changes in diet can influence microbiota compositions and impacts splenic leukocytes phenotype. With coexistence of imbalanced diets predominantly composed of n-6 fatty acids, we hypothesized that OBDs would cause dysbiosis in aging mice with alteration in splenic leukocyte profiling following MI in acute HF. The present study showed that OBD leads to an expansion of the genus *Allobaculum* with an expansion of neutrophils and disruption of neutrophil: lymphocyte ratio in aging. Thus, OBD dysregulated splenic immune cells with impaired interorgan immune metabolism and decreased immune-responsive $F4/80^+$ and $CD169^+$ macrophages with increased neutrophil swarming, which leads to the development of systemic inflammation in acute HF.

MATERIALS AND METHODS

Animal care and compliance

All animal MI surgery procedures and treatments were conducted according to the *Guide for the Care and Use of Laboratory Animals* [Eighth Edition, 2011; National Institutes of Health (NIH), Bethesda, MD, USA] and American Veterinary Medical Association (AVMA; Schaumburg, IL, USA) *Guidelines for the Euthanasia of Animals* (2013 edition) and were approved by the Institutional Animal Care and Use Committees at the University of Alabama at Birmingham.

Age-related study design and diet intervention protocol

Male C57BL/6J mice, 6 mo (young) and 18 mo (aging) old, were sourced from the National Institute of Aging colony (NIH) and were maintained with free access to water and maintained on standard diet (STD, ~4% safflower oil diet) and OBD (10% safflower oil) for 2 mo under a constant temperature of 19.8–22.2°C. Young adult and aging mice were randomized into 4 groups and designated as young-STD, young-OBD, aging-STD, and aging-OBD groups. The detailed study design is presented in **Fig. 1*A***.

Fecal sample collection and microbiome analysis

Aging colony acclimatized 2 wk before adding on diet protocol. A minor difference between the National Institute of Aging and The University of Alabama at Birmingham microbiota was noted. Fecal samples were collected in sterile tubes before the diet initiation and at the end of OBD and stored at −80°C before analyses. Microbial genomic DNA was isolated using a Fecal DNA Isolation Kit from Zymo Research (Irvine, CA, USA) following the manufacturer's instructions. Once the sample DNA was prepared, PCR was used with unique barcoded primers to amplify the variable region 4 of the 16S rDNA gene to create an amplicon library from individual samples (23, 24). The PCR product of ~255 bases from the variable region 4 segment of the 16S rDNA gene was sequenced using single-end reads using the MiSeq (Illumina, San Diego, CA, USA) followed by quality (23). To support the analysis of microbiome data, we have established an analytical pipeline (24, 25) based on the latest version of the Quantitative Insights Into Microbial Ecology (QIIME) tool suite (26). The first step in our analysis was to assess the quality of the raw data using FastQC, and then low-quality data was filtered out using the FastX toolset (StarNet, Santa Clara, CA, USA). The Ribosomal Database Project (Michigan State University, East Lansing, MI, USA) classifier trained using the Greengenes (v.13.8) 16S rRNA gene database was used to make taxonomic assignments for all operational taxonomic units (OTUs) at confidence threshold of 80% (0.8). The resulting OTU table included

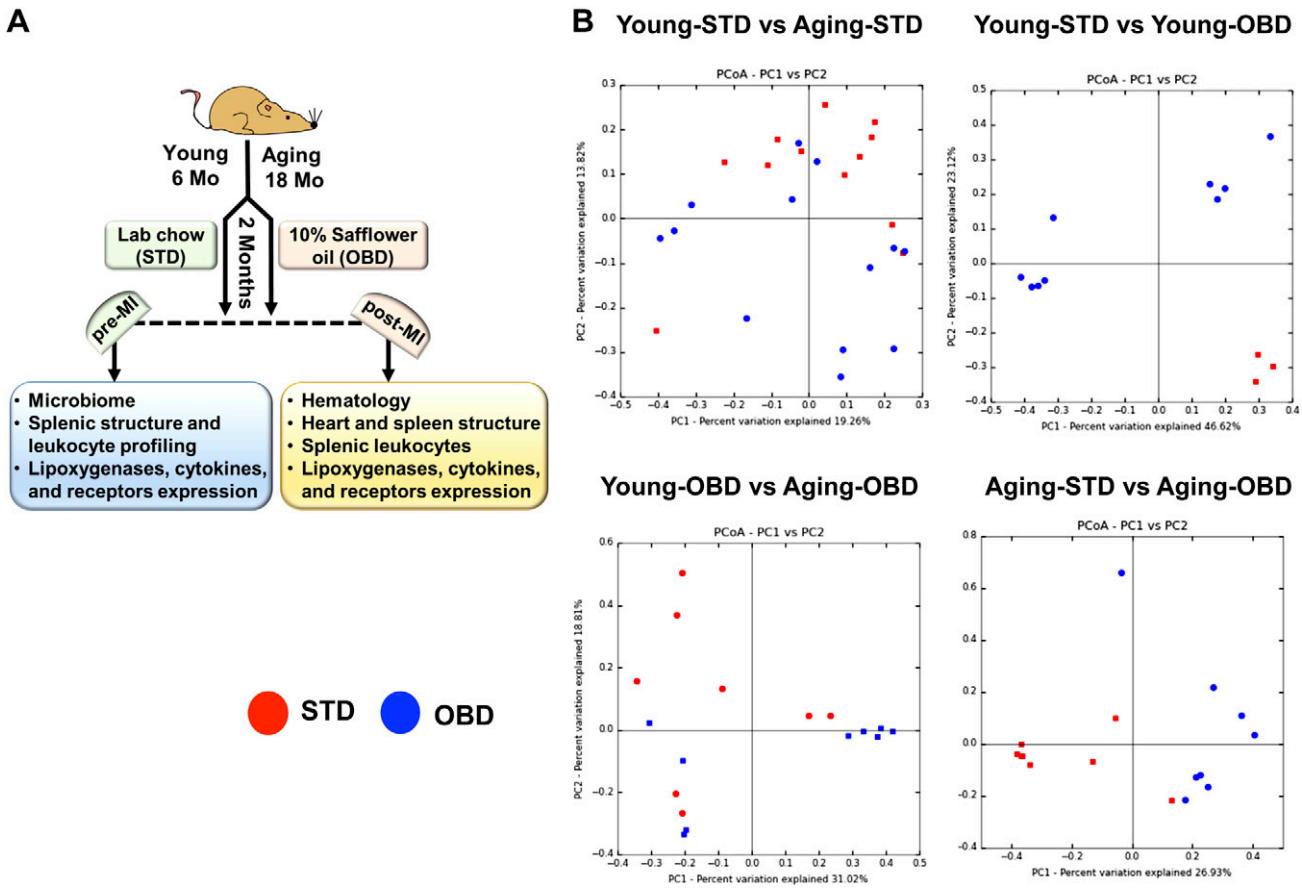

Figure 1. Impact of OBD on gut microbiota during aging. *A*) Study design sketch that delineates C57BL/6 mice age, diet intervention protocol, and parameters studied before and after MI in acute HF. *B*) PCoA plot of Bray-Curtis (n = 3–8 mice/group).

all OTUs, their taxonomic identifications, and abundance information. OTUs whose mean abundance was <0.005% were filtered out. OTUs were then grouped together to summarize taxon abundance at different hierarchical levels of classification (*i.e.*, phylum, class, order, family, genus, and species). These taxonomy tables were also used to generate stacked column bar charts of taxon abundance using Microsoft Excel software (Microsoft, Seattle, WA, USA). Alpha diversity (within sample diversity) was calculated using Shannon's metrics as implemented in QIIME. β-Diversity (between sample diversity) among different samples was measured using weighted UniFrac metrics. Principal coordinates analysis (PCoA) was performed by QIIME to visualize the dissimilarity matrix (β-diversity) between all the samples. Three-dimensional PCoA plots were generated using Emperor (23).

Coronary ligation surgery

Young and aging mice without surgery were maintained as d 0 naive controls. To induce acute HF, mice were subjected to permanent surgical occlusion of the left anterior descending coronary artery, as previously described in refs. 27 and 28. The mice were monitored after surgery until MI d 1 (24 hrs) for necropsy.

Hematology

For determination of complete blood counts, blood was collected from heparin-injected mice during necropsy (28). Complete blood count was determined using an automatic veterinary hematology analyzer (Hemavet 950 FS; Drew Scientific, Miami Lakes, FL, USA).

Left ventricle and spleen histology using hematoxylin and eosin staining

Post-necropsy, the paraffin-embedded left ventricle (LV) and spleen transverse sections were initially deparaffinized and then stained with hematoxylin and eosin. Total 5–7 images per slide per mouse were captured using an imaging microscope (Olympus, Tokyo, Japan).

Confocal microscopy

For immunofluorescence imaging, spleen cryosections were fixed, permeated, and blocked and then incubated with antibody against F4/80 (green) and CD169 (red) overnight. In addition, incubated with secondary antibody were conjugated with Alexa Fluor 555 and Alexa Fluor 488 for 1 h. Nuclei were stained with Hoechst. Confocal imaging microscopy was performed on a Nikon A1 high-resolution microscope (Nikon, Tokyo Japan), and images were acquired according to standard protocols. The images are representative of a 7–8 section area for 3–4 mice per group.

Flow cytometry

Single mononuclear cells were isolated from spleens of young-STD, young-OBD, aging-STD, and aging-OBD mice, and

leukocytes were profiled by flow cytometry. In brief, splenocyte count was adjusted to ~1–2 million mononuclear cells per stain. Isolated cell suspensions were finally suspended in 200 μl 1:500 Fc block and incubated for 10 min on ice. A cocktail of fluorophore-labeled mAb in 2× concentration was added for 30 min on ice as appropriate for each study. We used CD45-phycoerythrin (BD Biosciences, San Jose, CA, USA), CD11b-APC, F4/80-Percp (Thermo Fisher Scientific, Waltham, MA, USA), lymphocyte antigen 6 complex, locus C (Ly6C)–FITC (BD Biosciences), and Lymphocyte antigen 6 complex locus G (Ly6G)–pacific blue (eBioscience, San Diego, CA, USA) in a cocktail. All the population was primarily gated using $CD45^+$ markers for hematopoietic cells. The neutrophils were defined as $CD11b^+$ and $Ly6G^+$ cells. Activated macrophages were defined as the cells having dual expression of CD11b (macrophage-1 antigen) and $F4/80^+$ surface marker. Data were acquired on LSR II flow cytometer (BD Biosciences) and analyzed with FlowJo software, v.10.0.8 (BD Biosciences) (29).

Measurement of isoprostanoid markers using liquid chromatography–tandem mass spectrometry

Isoprostanoids (such as 15-F2t-IsoP) derived from nonenzymatic free-radical peroxidation of polyunsaturated fatty acids are excellent markers of lipid peroxidation *in vivo* and more generally of oxidative stress (30). Isoprostanoid quantification by liquid chromatography–mass spectrometry (LC-MS) currently represents a significant, specific, and noninvasive method for lipid peroxidation evaluation. This study consisted of an LC-MS profiling of mainly F2-IsoPs (15- and 5-series) derived from arachidonic acid (C20:4 n-6) in plasma.

Isoprostanoid measurements

After extraction of the lipids, oxidative damage to lipids was measured by levels of isoprostanoids in plasma, based on microliquid chromotography–tandem mass spectrometry (LC-MS/MS) (31, 32). The first step consisted of an alkaline hydrolysis of samples, allowing the global quantification of compounds (free and bound forms). Then, metabolites were concentrated thanks to a solid phase extraction step conduced on weak-anion exchange materials. There with metabolites were analyzed by micro–LC-MS/MS. Mass spectrometry analyses were performed in a QTrap 5500 (Sciex, Framingham, MA, USA). The ionization source was electrospray in negative mode. Detection of the fragmentation ion products from each deprotonated molecule $(M\text{-}H)^-$ was performed in the multiple reaction monitoring mode. Concentration of the analytes was obtained by calibration curves calculated by the area ratio of the analytes and the internal standard. Data processing was achieved using the MultiQuant 3.0 software (Sciex) (30–32).

Real-time quantitative PCR for measurements of gene transcripts

For quantitative PCR (qPCR), RT was performed with 2.0 μg of total RNA using SuperScript Vilo cDNA Synthesis Kit (Thermo Fisher Scientific). qPCR for arachidonate 12-lipoxygenase (LOX) (*Alox-12*), arachidonate 15-LOX (*Alox-15*), arachidonate 5-LOX (*Alox-5*), *IL-1β*, *TNF-α*, C-C motif chemokine ligand 2 (*Ccl2*), arginase 1 (*Arg-1*), mannose receptor C-type 1 (*Mrc-1*), chitinase-like protein 3 (*Ym-1*), formyl peptide receptor (*FPR*) 2, G-protein coupled receptor (*GPR*) 40, and *GPR120* genes was performed using TaqMan probes (Thermo Fisher Scientific) on a Master Cycler ABI, 7900HT. Gene levels were normalized to hypoxanthine phosphoribosyltransferase 1 as the housekeeping control gene. The results were reported as $2^{-\Delta Ct}$ ($\Delta\Delta C_t$) values. All the experiments were performed in duplicates with $n = 5$ mice per group.

Statistical analysis

For the microbiome analysis, samples were grouped by user-defined variables, and significant differences between groups were determined by performing a permutational multivariate ANOVA test on each of the β-diversity indices. Furthermore, a Kruskal-Wallis test was performed to identify key taxa whose changes in relative abundances between groups are playing a significant role in driving the overall group differences. These statistical tests are performed using tools within the QIIME package. Data are expressed as means ± SEM. Statistical analyses were performed using Prism 7 (GraphPad Software, La Jolla, CA, USA). Two-way ANOVA was used for comparisons between young-STD, young-OBD, aging-STD, and aging-OBD. A value of $P < 0.05$ was considered as statistically significant.

RESULTS

Gut microbe community differences between young and old mice fed OBD compared with STD

C57BL/6 mice (young; 6 mo and aged 18 mo) were fed the STD (4% safflower oil) and OBD (10% safflower oil) for 2 mo. To evaluate the effect of OBD on the intestinal microbiome composition, we examined the microbes in the individual fecal samples obtained from the groups of mice fed STD and OBD using 16S rRNA gene sequencing. Irrespective of age, OBD independently increased actinobacteria. A pie chart displayed the actinobacteria percentage at 5% higher in young-OBD than young-STD mice. In aging, the percentage of actinobacteria in OBD increased a further ~8%, with no change in aging mice fed STD (Supplemental Fig. S1). Composition analysis using unweighted and weighted UniFrac revealed no microbiome composition differences between young mice (6 mo of age) and older mice (18 mo of age) ($P > 0.05$), whereas a difference was seen using Bray-Curtis ($P < 0.02$) (Fig. 1*B*). In contrast, comparison of young or aging mice found significant differences between the STD and OBD with Bray-Curtis and unweighted and weighted UniFrac. However, we also found no significant differences in microbe composition between the young or old mice fed the OBD.

We next examined the relative abundance of the gut microbes in the young and old mice fed the different diets (**Fig. 2**). With the exception of a single mouse (X49/AF), we did not observe a dysbiosis with a dominant microbe in the young or old mice fed the STD or OBD. Both young and aging STD-fed mice displayed highest relative abundance of *Bacteroides* family S24-7, which has been found many times to be the predominant microbe in mice (33). A Kruskal-Wallis test confirmed that the S24-7 was ~2-fold higher in both the young and old animals fed the STD than those fed OBD (Supplemental Tables S1–S3). In contrast, for both young and old mice fed OBD, the genus *Allobaculum* was the most abundant microbe. A Kruskal-Wallis test revealed that this microbe was between 4- and 8-fold

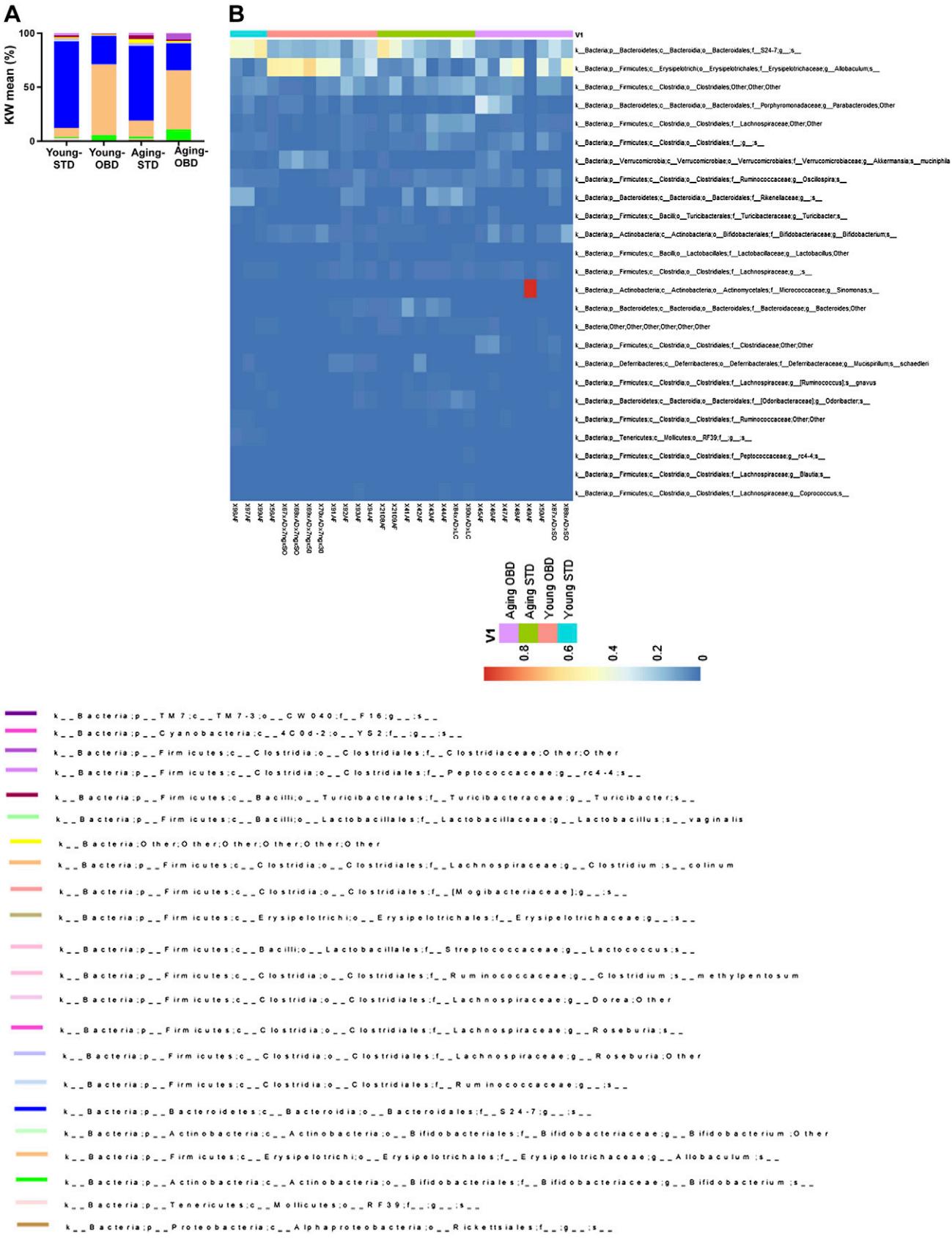

Figure 2. Impact of OBD and aging on distribution of microbiota taxa. *A*) Relative abundance by Kruskal-Wallis (KW) mean of the top bacterial phyla. *B*) Heatmap showing the abundance of significant OTUs. Represented bacterial taxa information (genus, family, and phylum) of these OTUs is also shown (n = 3–8 mice/group).

higher in mice fed the OBD rather than STD. Blasting of the OTU for this microbe against the National Center for Biotechnology Information (Bethesda, MD, USA) database revealed that it is most probably *Faecalibaculum rodentium*, which has previously been isolated from mice and has been found to increase in abundance in mice fed diets rich in fat (34). Collectively, the microbiome analysis demonstrates that OBD drastically changes the overall gut microbe composition from mice fed the STD regardless of age.

OBD-fed aging mice displayed feed-forward systemic inflammation with the expansion of neutrophils

To determine whether these differences in the microbiota correlated with changes in the systemic immune population, we performed hematologic analyses of blood in all 4 groups. The clinical hematology analyses of mouse blood showed that the immune composition was as follows: lymphocytes and neutrophils (40 and 44%, respectively), followed by monocytes (10%), eosinophils (5%), and basophils (1%) in young mice fed STD. The OBD-fed young mice increased neutrophils to 62% and reduced lymphocytes to 29%. Independent of diet, aging alone increased neutrophils to 67% and decreased lymphocytes to 29% compared with young mice fed STD in which neutrophils were 44% and lymphocytes were 40%. The OBD-fed aging mice displayed similar composition of neutrophils and lymphocytes as displayed by STD aging mice (**Fig. 3*A***). The hematologic analysis displays that aging is a primary variable that increased neutrophils and decreased lymphocytes, monocytes, eosinophils, and basophil populations (Fig. 3*B–F*). These results suggest that OBD increased neutrophils, indicative of systemic inflammation with major influence from microbiome and aging.

OBD-fed mice develop splenic structural deformity in aging

Young-STD mice spleens displayed physiologic architecture composed of red pulp (RP) and white pulp (WP) regions surrounded by a fibrous capsule; the WP is surrounded by the splenic marginal zone (MZ) (Supplemental Fig. S2*E*). Histologic analysis revealed that aging-STD mice showed significant structural disorganization.

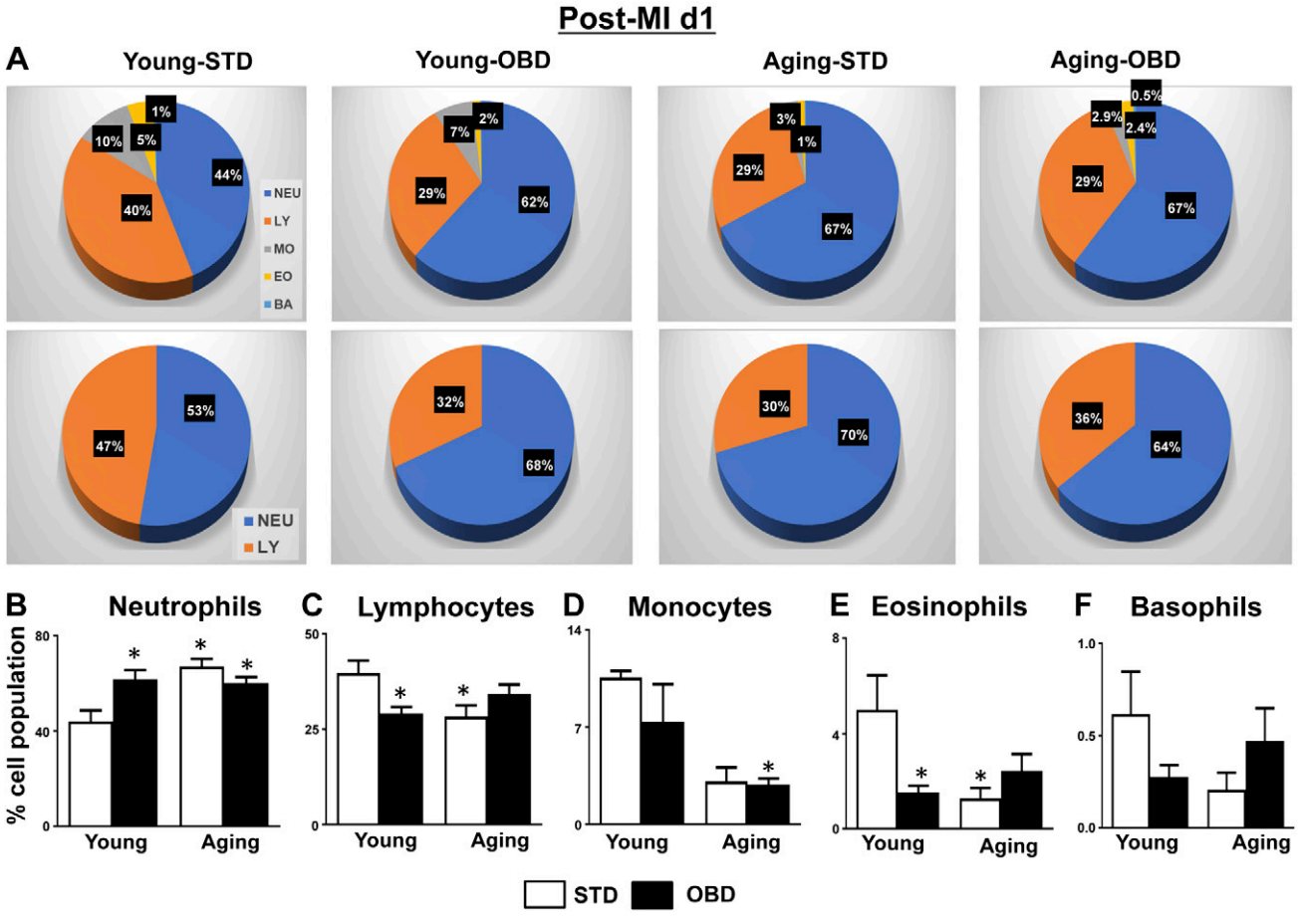

Figure 3. Aging and OBD impacted on hematology profile post-MI. *A*) Pie chart displaying white blood cell differential of in young and aging mice fed STD and OBD for 2 mo. Bar graphs represent % of *B. B–F*) Neutrophil (*B*), lymphocyte (*C*), monocyte (*D*), eosinophil (*E*), and Basophil (*F*) population in blood of young and aging mice fed STD and OBD for 2 mo post-MI. BA, basophil; EO, eosinophil; LY, lymphocyte; MO, monocyte; NEU, neutrophil. Values are means ± SEM (n = 8–10 mice/group). *$P < 0.05$ *vs.* young-STD.

STD-fed aging mice spleen WP was shrunken with less-defined boundaries, and further MZ macrophages were disrupted, no longer forming a continuous boundary along the MZ (Supplemental Fig. S2*G*). Young-OBD mice spleen had a structure with limited pathophysiological changes (Supplemental Fig. S2*F*). However, the aging-OBD mice displayed an expansion of WP area, with discontinuous MZ (Supplemental Fig. S2*H*). At the structural level, LV tissue did not display any histologic or pathologic changes indicative of limited impact of diet and aging (Supplemental Fig. S2*A–D*). Thus, spleen and LV morphology results suggest that OBD induced structural disorganization of spleen in aging mice.

OBD-fed mice revealed deranged splenic MZ and WP in aging post-MI

The spleen serves as a leukocyte reservoir in the event of a cardiac injury and stroke or infection and mobilizes leukocytes to heart in response to the tissue repair process to facilitate resolution of inflammation (35). LV structural changes confirmed post-MI pathology in young and aging mice fed on STD and OBD diet (Supplemental Fig. 3*A–D*). Therefore, the splenic structure and morphology were evaluated to determine the effect of the interaction between a fatty acid–enriched diet and aging. Post-MI, the WP area was observed to be expanded with irregular deformation, and MZ was shrunken in aging-STD fed mice compared with young-STD fed mice (Supplemental Fig. S3*E–F*). The OBD-fed young and aging mice display deranged WP and MZ (Supplemental Fig. S3*G*, *H*) with minimal expansion of RP zone. Thus, histologic evaluation of spleen post-MI explained the deformation of WP area was prominent because of diet but independent of MI and aging.

OBD impaired splenic metallophilic macrophage F4/80$^+$ and CD169$^+$ in aging

The splenic RP contains macrophages (CD169) and stromal cells, which are important in the clearance of pathogens, and deficiency can lead to multi-organ damage in infection (36, 37). Thus, to understand the impact of age and OBD on metallophilic macrophages (CD169), we performed immunofluorescence staining. Confocal imaging of spleen showed presence of F4/80$^+$(green) in WP, MZ, and RP area with the presence of CD169$^+$(red) metallophilic macrophages in the MZ (Supplemental Fig. S4*A*). The OBD-fed young mice showed the sporadic and deranged distribution of F4/80$^+$ macrophages with reduced density of the CD169$^+$ cells (Supplemental Fig. S4*B*). Because of aging-STD, the WP area was shrunken, with a higher expression F4/80$^+$ macrophages and uneven distribution of CD169$^+$, both F480$^+$ and CD169$^+$ were colocalized (yellow) in splenic morphology (Supplemental Fig. S4*C*). Thus, OBD in aging mice impacted the expression and distribution of CD169$^+$ macrophages, which appeared to move toward WP area and form uneven colonies (Supplemental Fig. S4*D*). Post-MI, WP area expanded both in young and aging mice with irregular demarcations. Both STD-fed young and aging mice displayed prominent expression of F4/80$^+$ and CD169$^+$ (**Fig. 4*A*, *C***) when compared with OBD. Interestingly, OBD impacted the loss of CD169$^+$ expression compared with STD-fed mice, independent of aging (Fig. 4*B*, *D*). Thus, OBD serves as a prime factor in decreasing CD169$^+$ macrophages, indicative of splenic immune dysregulation in cardiac injury.

Aging limits splenic macrophages in OBD and STD groups

Quantitative analyses of leukocytes CD45$^+$ and CD11b$^+$ in spleen by flow cytometry showed no difference in the percentage population in young and aging mice maintained on STD in no-MI naive controls. The no-MI controls displayed lower percentage CD45$^+$ and CD11b$^+$ population in OBD aging mice, which had 0.30% monocytes compared with young-OBD mice, which displayed 5.61% of cells (**Fig. 5*A***). In response to cardiac injury, there was a global increase in splenic CD45$^+$ and CD11b$^+$ population due to OBD, independent of age. Post-MI, the young and aging mice fed OBD showed increased percentage of CD11b$^+$ cells (9.22 $\pm$ 0.5 and 1.5 $\pm$ 0.2%; Fig. 5*A*) compared with young and aging cohorts fed STD, respectively, indicating OBD increases monocytes independently. The splenic CD11b$^+$ and F4/80$^+$ cells (macrophages) in young and aging mice fed STD displayed 0.62 $\pm$ 0.2 and 0.12 $\pm$ 0.01% (Fig. 5*B*) respectively. The young-OBD mice showed a 3.5-fold increase in the population of CD11b$^+$ and F4/80$^+$ macrophages compared with aging-OBD. Post–cardiac injury, there was an overall decrease in CD11b$^+$ and F4/80$^+$ in aging compared with young mice (Fig. 5*B*). Post-MI, splenic leukocytes were activated with CD11b$^+$ and F4/80$^+$ (2.2 $\pm$ 0.3%) in young-OBD mice compared with young-STD (0.62 $\pm$ 0.2%) mice (Fig. 5*B* and Fig. 5*D*). However, overall aging decreased both monocytes and macrophages in spleen compared with wild type. These results indicate age served as a diversified factor for splenic macrophages in acute HF. Aging undermines macrophage population in OBD- and STD-fed mice compared with young mice.

Aging impacts splenic leukocytes (macrophages, Ly6C$^+$ and neutrophils, Ly6G$^+$)

Splenic leukocytes (neutrophils and macrophages) are dysregulated in obese aging (27). Aging serves as a key factor in decreasing splenic CD11b$^+$, F4/80$^+$, low-Ly6C (Ly6C^{lo}), and high-Ly6C (Ly6C^{hi}) (macrophage phenotype) and CD11b$^+$, F4/80$^-$, and Ly6G$^+$ (neutrophils) population, irrespective of diet (**Fig. 6**). Macrophages polarize either toward reparative (Ly6C^{lo}) or proinflammatory (Ly6C^{hi}) phenotypes post-MI. No-MI control aging-OBD mice displayed a significant decrease in CD11b$^+$, F4/80$^+$, and Ly6C^{hi} (0.11 $\pm$ 0.02%) compared with young-OBD mice (1.11 $\pm$ 0.2%) in spleens (Fig. 6*A*), indicating that aging drives macrophage population independent of diet. The splenic leukocyte population of Ly6C^{hi} of aging OBD-fed mice (0.27 $\pm$ 0.1%) was lower than young OBD-fed mice (2.2 $\pm$ 0.2%) (Fig. 6*A*, *C*). Simultaneously, young-OBD mice displayed increased CD11b$^+$, F4/80$^+$, and Ly6C^{lo} (1.0 $\pm$ 0.1%) levels when

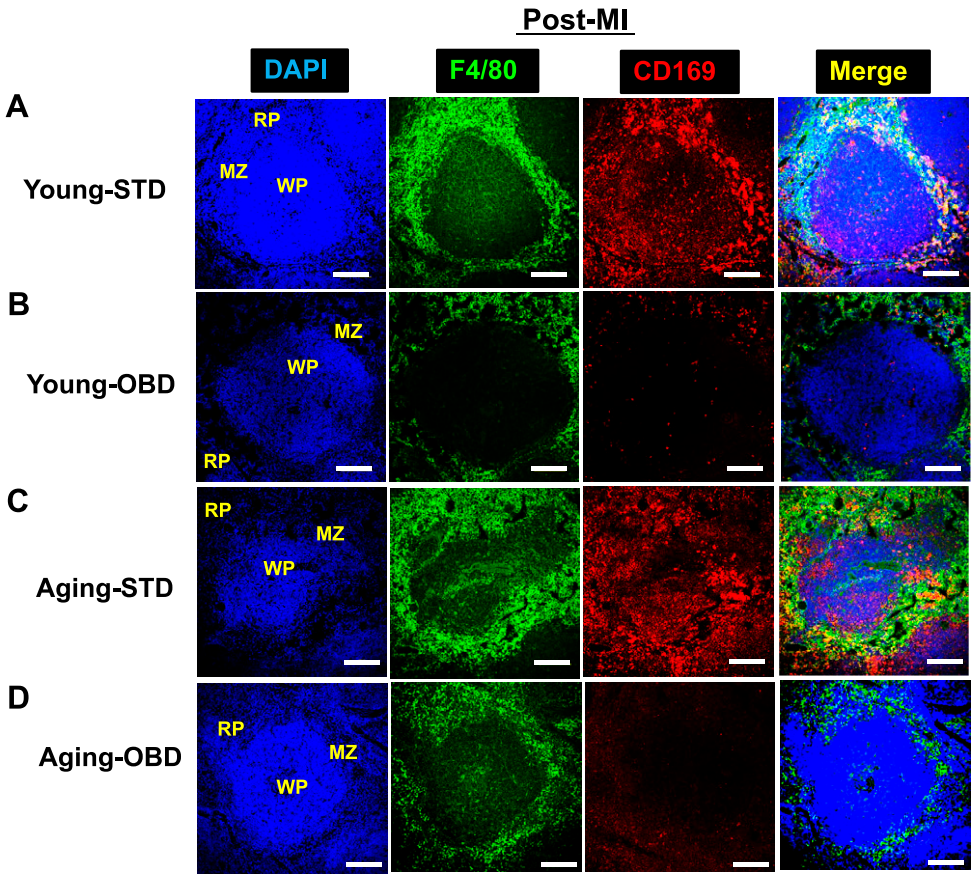

Figure 4. OBD decreased CD169$^+$ macrophages in young and aging mice post-MI. *A–D*) Immunofluroscence of post-MI spleen sections from young and aging mice fed normal diet and OBD, presenting 3-color image staining; CD169 (red), F4/80 (green), and nuclei (blue). OBD cleared CD169+ cells in WP and MZ area post-MI, with expansion of F4/80$^+$ in both young and aging mice. Images are representative of 4–5 sections, n = 4/group. Original magnification, ×20. Scale bars, 100 μm.

compared with aging-OBD (0.03 ± 0.01%) post-MI (Fig. 6*A, D*).

In naive controls, the young-STD mice showed a higher percentage (0.14 ± 0.01%) of neutrophils (Ly6G$^+$) than aging-STD (0.03 ± 0.01%) in the spleen. The young-OBD mice displayed recruitment of excess splenic neutrophils (CD11b$^+$ and Ly6G$^+$) (Fig. 6*B*). The OBD-fed mice showed a greater density of Ly6G$^+$ cells in young (3.2 ± 0.4%) and aging (0.7 ± 0.1%) mice post-MI d 1 in the spleen (Fig. 6*B, E*). Of note, the OBD-fed mice also displayed a higher expression of CD11b$^+$ and Ly6G$^+$ cells than STD post-MI in the spleen (Fig. 6*F*). The results indicate that aging served as a universal variable that overall decreases macrophages and neutrophil population in spleen; however, OBD highly impacted splenic leukocytes in young mice.

Aging altered splenic LOXs, cytokines, and GPCR expression, whereas OBD affected young mice

Immune-responsive LOXs are essential enzymes for healing that utilize the essential fatty acids to transform into the bioactive lipids that modulate immune kinetics (29). OBD-fed aging mice decreased splenic expression of *Alox-12* and *-15* (1.2- and 3-fold) and increased *Alox-5* (1.4-fold) compared with the young-STD mice. Post-MI, splenic mRNA levels on *Alox-12*, *-15*, and *-5* were increased in aging-STD mice compared with young-STD mice (**Fig. 7*A***).

To determine whether age and diet interact with splenic low-grade chronic inflammation, the expression levels of proinflammatory and reparative cytokines were evaluated. Post-MI, STD-fed aging mice had increased *IL-1β* compared with all other groups, indicative of an inflamed spleen. Despite increased *IL-1β*, the *Tnf-α* encoding genes were not changed in all the groups. However, *Ccl2* levels were increased in the young-OBD group but decreased in aging-OBD, indicative of differential effects of OBD in young and aging mice (Fig. 7*B*). The reparative cytokines *Mrc-1*, *Arg-1*, and *Ym-1* were increased in splenic expression in STD-fed aging mice compared with all other groups (Fig. 7*C*).

As OBD activated, multiple metabolite-sensing GPCRs lead to the formation of lipid mediators, and therefore splenic expression of receptors FPR2, GPR120, and GPR40 were determined pre- and post-MI. In no-MI controls, aging-OBD mice displayed higher expression of FPR2 than young-STD, young-OBD, and aging-STD. Post-MI, the young mice fed STD and OBD elicited FPR2 expression in the spleen compared with no-MI respective controls. Splenic GPR40 expression was decreased in young-OBD no-MI control compared with young-STD mice. Similar to FPR2, the aging mice fed STD and OBD displayed a decrease in GPR40 compared with young mice fed STD and OBD post-MI. Inversely, splenic expression of GPR120 was down-regulated post-MI in the young and aging mice (STD and OBD mice) compared with the no-MI respective control group (Fig. 7*D*). Thus, the above results suggest that aging and diet are dependable factors impacting immune-responsive LOXs, cytokines, and metabolite-sensing receptor signaling in acute HF.

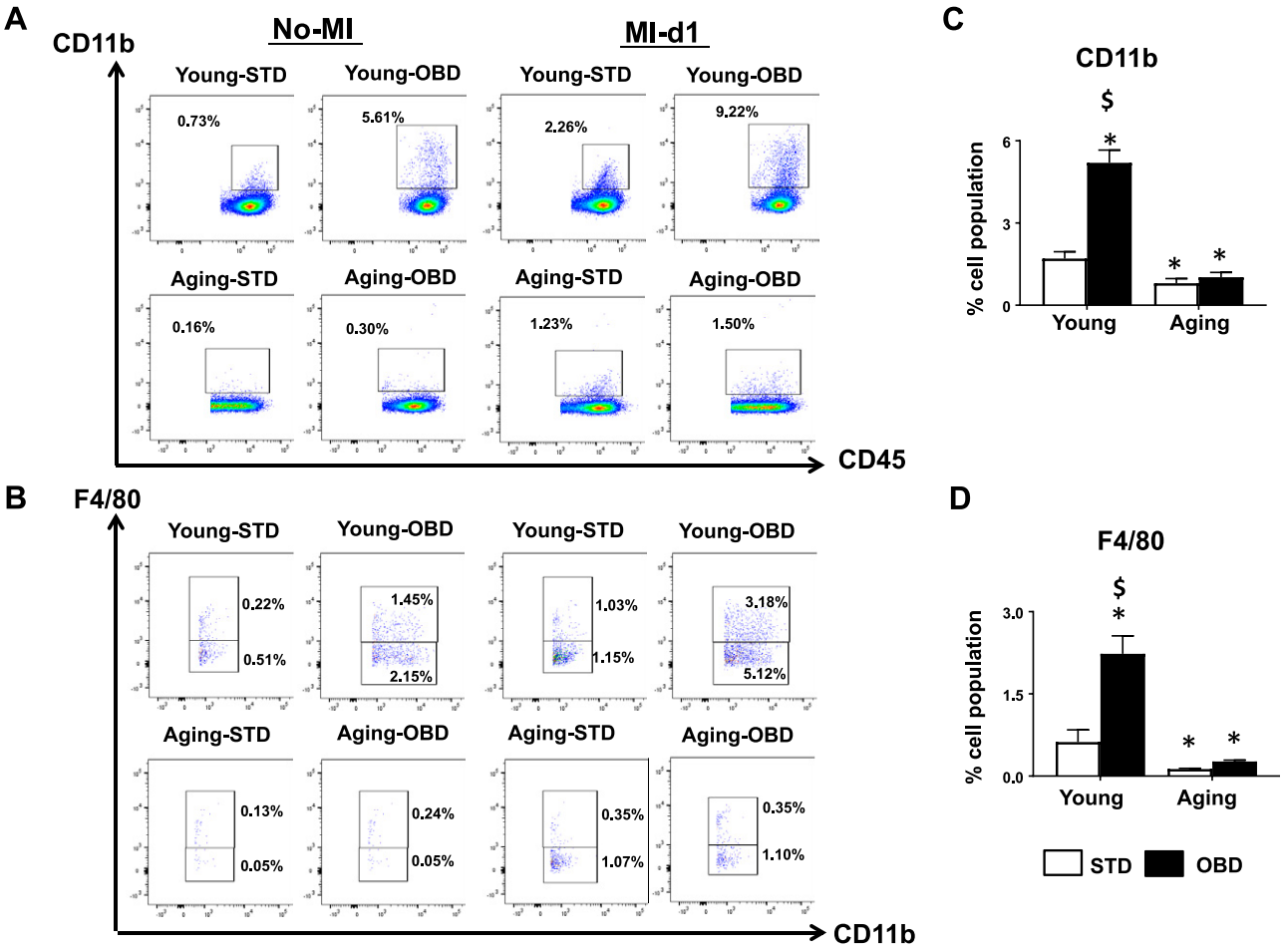

Figure 5. Aging diminished splenic leukocyte kinetics independent of OBD post-MI. *A*) Representative flow cytometry dot plots depicting $CD45^+/CD11b^+$ population in spleen isolated from young and aging mice fed STD and OBD for 2 mo pre- and post-MI. *B*) Representative flow cytometry dot plots showing lower $CD11b^+/F4/80^+$ population in spleen isolated from young and aging mice fed STD and OBD for 2 mo pre- and post-MI. *C*) Bar graphs representing percentage of $CD11b^+$ population in spleen at d 1 post-MI. *D*) Bar graphs representing percentage of F4/80+ population in spleen at d 1 post-MI. Values are mean ± SEM (n = 3–5 mice/group/time point for flow cytometry analysis). $^*P < 0.05$ *vs.* young-STD, $^{\$}P < 0.05$ STD *vs.* OBD.

OBD increases plasma isoprostanoids independent of aging post-MI

Isoprostanes (such as 15-F_{2t}-IsoP) derived from nonenzymatic free-radical peroxidation of polyunsaturated fatty acids are excellent markers of lipid peroxidation *in vivo* and, more generally, of oxidative stress (30). Analyses of plasma isoprostanoids revealed F_2 isoprostanes [15-F_{2t}-IsoP, 15-epi-15-F_{2t}-IsoP, and 5(*RS*)-5-F_{2t}-lsoP] were decreased in aging post-MI compared with young mice fed STD (**Fig. 8*A*–*C***). However, OBD independently increased the levels of 15-F_{2t}-IsoP, 15-epi-15-F_{2t}-IsoP, and 5(*RS*)-5-F_{2t}-lsoP, suggesting an excess intake of OBD increased isoprostanoids post-MI, which is indicative of amplified lipid peroxidation.

DISCUSSION

Dietary metabolites interact with gastrointestinal microflora to calibrate leukocyte defense capacity, thereby creating a feed-forward and feed-back system between diet and health (7). The importance of diet metabolite interaction with the microbiome is essential to train the leukocyte defense system. The consumption of n-6 polyunsaturated fatty acids (PUFAs) (in the United States increased from ~3 to 7.21% of energy (38). The impact of dietary macronutrient and micronutrient influence on immune cells differs during young and aging and drastically impacts cardiac health (27, 39). However, how OBD influences microbiota during aging, leukocyte kinetics, and cardiac health is underinvestigated. Therefore, in the present study, we defined the intestinal microbiota, interorgan connection of splenic structural remodeling with gut microbiota, and leukocyte profiling, because splenic leukocytes are essential for cardiac healing in the event of acute HF (35). The current study shows data from the widely used laboratory C57BL/6 mouse strain suggestive of polygenic settings necessary for human translational studies because similar calorie-dense diets are consumed in humans. Here, we precisely used a single fatty acid–enriched diet (10% safflower oil; w/w) that mimicks a standard Americanized Western diet, indicating the differential impact of same diet in young and aging settings. The study discovered that aging superimposed with OBD

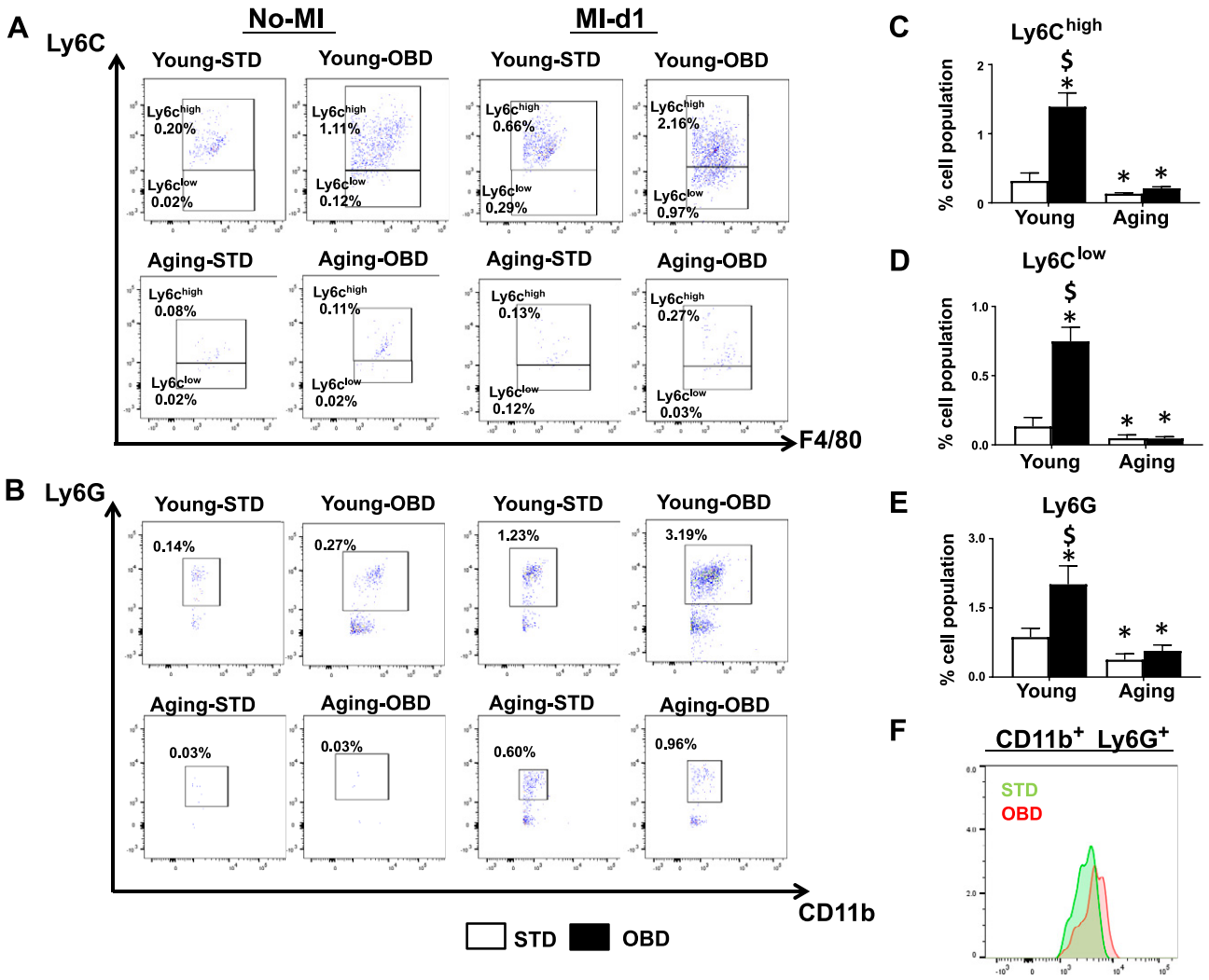

Figure 6. Aging diminishes F480$^+$ and Ly6C^{hi} and Ly6G$^+$ cells post-MI irrespective having excess intake of fatty acids. *A*) Representative flow cytometry dot plots depicting Ly6C^{hi} and Ly6C^{lo} population in spleen isolated from young and aging mice fed STD and OBD for 2 mo pre- and post-MI. *B*) Representative flow cytometry dot plots showing LY6G population in spleen isolated from young and aging mice fed STD and OBD for 2 mo pre- and post-MI. *C*) Bar graphs representing % of Ly6G population in spleen at d 1 post-MI. *D*) Bar graphs representing % of Ly6C^{lo} population in spleen at d 1 post-MI. *E*) Bar graphs representing % of Ly6G population in spleen at d 1 post-MI. *F*) Histogram representing change in Ly6G expression in aging mice fed STD and OBD for 2 mo post-MI. Values are means ± SEM (n = 3–5 mice/group/time point for flow cytometry analysis). *$P <$ 0.05 *vs.* young-STD, $^{\$}P < 0.05$ STD *vs.* OBD.

lead to dysbiosis and highlighted the miscalibration of splenic leukocytes, leading to nonresolving inflammation. Thus, OBD was enriched in aging; led to dysbiosis with expansion of genus *Allobaculum*; expanded systemic inflammation with neutrophil swarming post-MI; dysregulated splenic leukocyte profiling in with decrease in CD169$^+$ macrophages in aging post-MI; and served as a determinent factor with marked dysregulation of cytokines and receptor expression pre- and post-MI (Fig. 8*D*).

Dysbiosis or altered microbes appear to be involved in the pathogenesis of diverse diseases such as obesity, insulin resistance, β-cell function, diabetes, hypertension gastrointestinal diseases, and related cardiovascular diseases, including HF (40–42). However, aging has been associated with dysbiosis-dependent mechanisms that lead to changes in ratios of Firmicutes and Bacteroidetes population, impacting immune modulation (43, 44). Previous reports have shown that obesity correlates with a shift in the abundance of Bacteroidetes and Firmicutes using monogenic mouse models such as *ob/ob* and *db/db* with profound signs of inflammation and dysbiosis (8, 22). However, how the pathogenicity of OBD leads to dysbiosis in aging in acute HF is covered in this report. For this, we used 10% w/w safflower oil enriched OBD that expanded the rare taxa, *Allobaculum*, disrupting the overall FIRM:CFB (Firmicutes:Bacteroidetes) ratio. The increase in the *Allobaculum* and *Bifidobacterium* correlated with the OBD. The *Bifidobacterium spp*. have been reposted to improve glucose homeostasis, reduce weight gain and fat mass, and improve insulin secretion in mice fed a high-fat diet (45). Studies have shown that oral supplementation with *Bifidobacterium* increased lymphocyte proportions in the circulation, improved the anti-tumoricidal activity, and restored phagocytosis in peripheral blood mononuclear

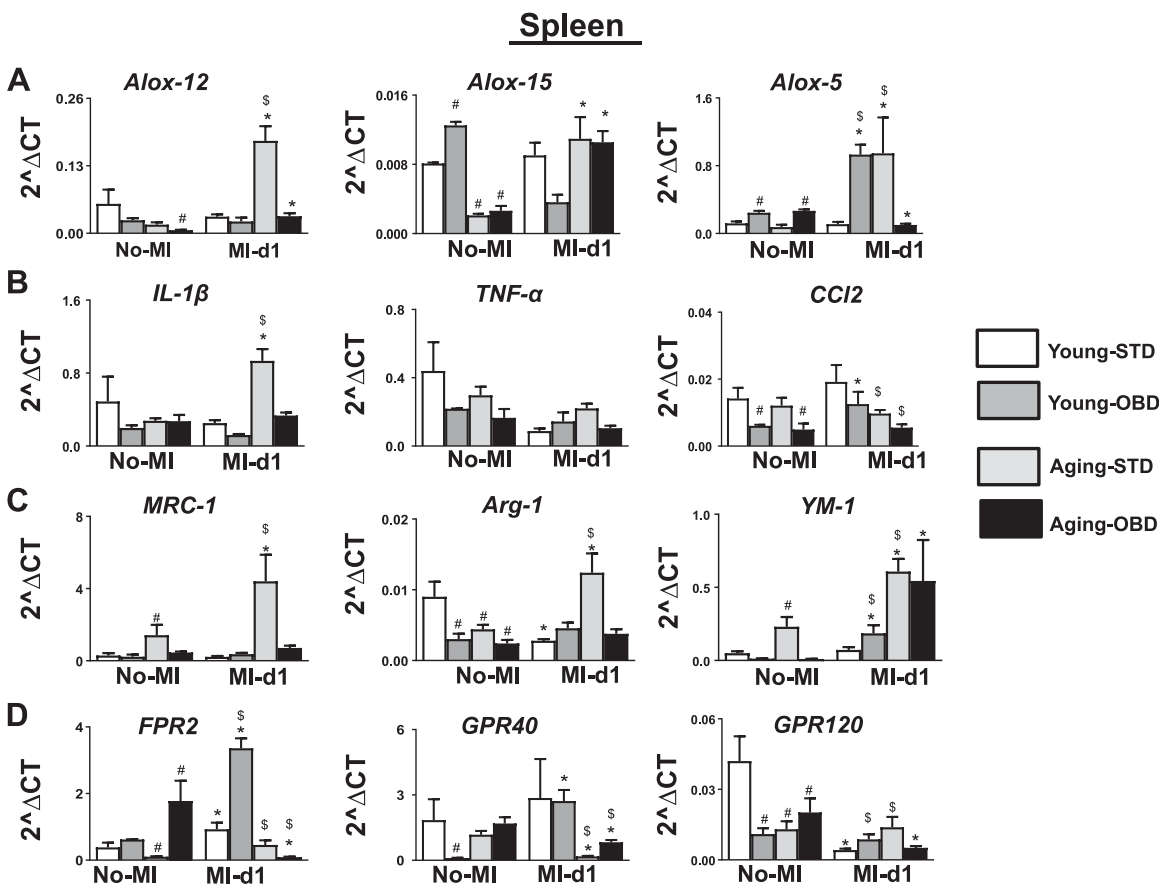

Figure 7. OBD modulates splenic LOXs, cytokines, and metabolite-sensing receptor expression in young and aging mice post-MI. Bar-graph representing mRNA expression of *ALOX-12*, *ALOX-15*, and *ALOX-5* (*A*); *IL-1b*, *TNF-α*, and *CCL2* (*B*); *MRC-1*, *Arg-1*, and *YM-1* (*C*); and *FPR2*, *GPR40*, and *GPR120* (*D*). Gene Expressions are normalized to hypoxanthine phosphoribosyltransferase 1 (*HPRT-1*) expression. Values are means ± SEM ($n = 4$/group). $^{\#}P < 0.05$ *vs.* young-STD no MI, $^{*}P < 0.05$ *vs.* young-STD post-MI, $^{\$}P < 0.05$ STD *vs.* OBD.

cells and neutrophils (46, 47). This indicates the compensatory mechanism because OBD, as well as aging acute HF, leads to an increase in neutrophils, with a decrease in total circulating lymphocytes and other leukocyte population intensifying the overall immune response. Overall, OBD promoted actinobacteria density pre-MI and disturbed the ratio of the microbiome, thereby influencing the defensive immune response and systemic inflammation in acute HF.

Diet and age are interactive factors that define microbiota, which leads to an imbalance in host defense of immune cell health in homeostasis and disease pathology. Diet interaction within the gut defines proximal, distal, and systemic inflammation, which in turn defines interorgan communication. The spleen is a secondary lymphoid organ and serves as a reservoir for the immune cells, regulating host defense or cardiac healing responses specifically in the event of HF (35, 39). The spleen is composed of RP and WP, which are separated by an interface, the MZ. The splenic RP zone consists of phagocytic macrophages that are critical for maintenance of blood homeostasis of senescent erythrocytes and in response to major injury such as MI, stroke, or infection (37, 48). Splenic MZ also contains macrophages and metallophilic macrophages that express a unique set of pattern-recognition receptors (CD169) to orchestrate innate immune response in infection and injury (37). $CD169^{+}$ macrophages can control parasite propagation and restrain inflammation, and their absence lead to multiorgan damage (36). In aging mice, OBD developed splenic WP shrinkage with less-defined boundaries. Splenic MZ had altered distribution, no longer forming a continuous boundary, indicating the defective homeostasis in MZ and myeloid cells. Further imbalance in splenic immune response due to the obesogenic environment was due to lowered CD169 macrophages in acute HF. $CD169^{+}$ splenic MZ macrophages are known to prime host defense and are essential to control damage-induced inflammation (37, 49). The decrease in CD169 expression post-MI is indicative of obesogenic environment influences and $CD169^{+}$ cells as well as splenic architecture that miscalibrates the immune response in acute HF.

Our data indicate that OBD in aging dysregulated splenic leukocytes with the expansion of systemic inflammation and the beginning of the incomplete resolution of inflammation in acute HF (35). The age-induced dysregulation in the innate immune system has been well established (27, 50). Our previous study has shown that aging mice without HF have a proinflammatory environment that results in a low-grade inflammation setting

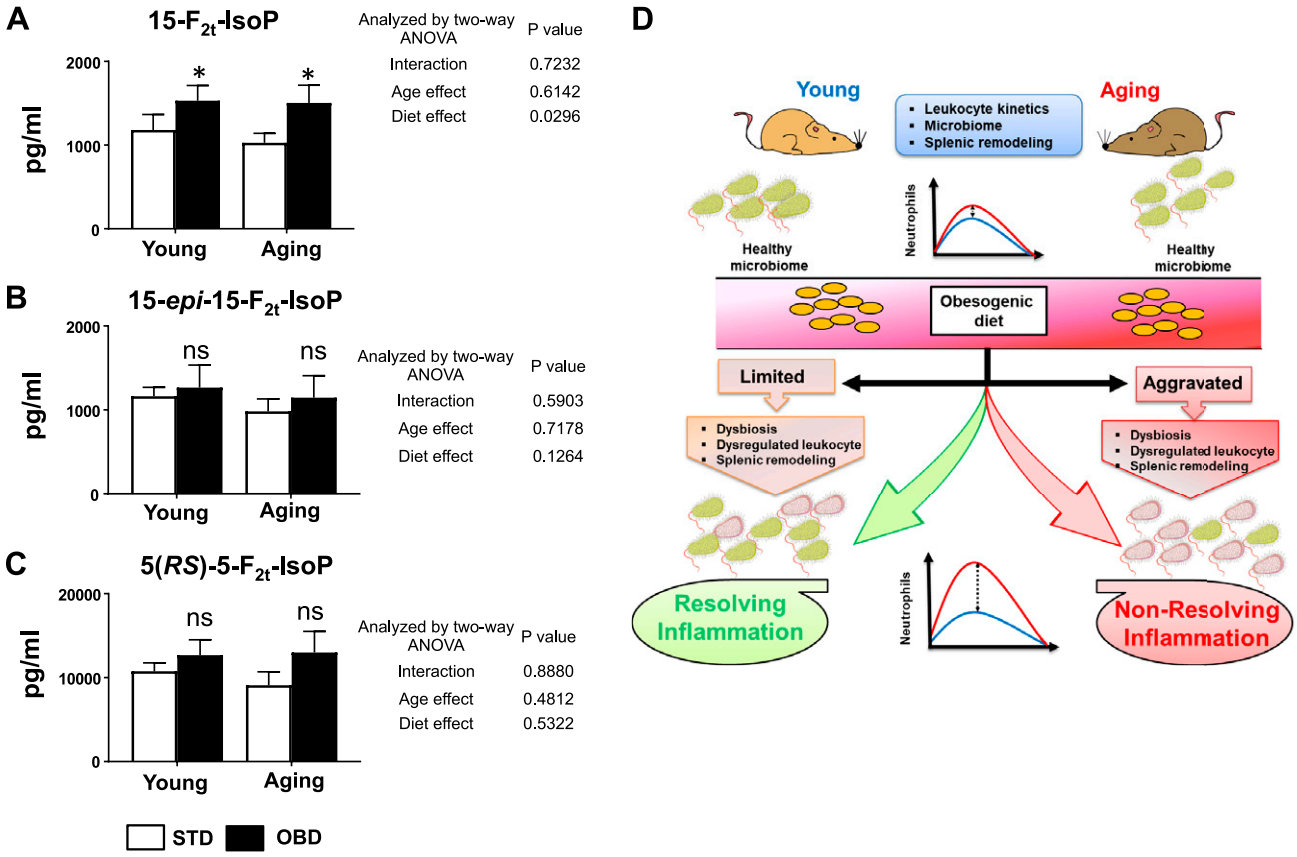

Figure 8. OBD modulates plasma level of isoprostanes. *A–C*) Bar graphs representing plasma level of 15-F_{2t}-IsoP (*A*), 15-epi-15-F2t-IsoP (*B*), and 5(*RS*)-5-F_{2t}-IsoP (*C*). *D*) The study outcome illustrating impact of OBD on gut microbiome and its impact on systemic inflammation.

that alters electrical and cardiac physiology (39). Examination of the splenic population in aging displayed a drastic decrease in all splenic leukocytes. Compared with humans, mouse blood is dominated by lymphocytes (B and T cells) (10), but OBD increases neutrophil swarming in both young and aging mice. In mice and humans, risk factors like aging or prolonged use of painkillers primes the neutrophil count in the blood (27, 51). Neutrophils are essential to resolve inflammation; however, sustained long-term neutrophil activation in circulation may lead to unstable angina (52). Clinical studies with increased neutrophil counts indicate a substantially increased risk for major adverse cardiovascular events, adding to the prognostic information of cofounding factors and other parameters of inflammation (53). Furthermore, a study has shown that immune cells such as mast cells, monocytes, neutrophils and platelets interact with isoprostanes leading to inflammation-induced thrombosis disorders (54). F_2-isoprostanes are involved in severe acute or chronic inflammatory diseases such as rheumatic diseases, asthma, and risk factors of atherosclerosis, diabetes, ischemia-reperfusion, and septic shock (55). Our study indicated OBD increased F_2-isoprostanes in both young and aging populations, indicative of an increase in lipid peroxidation and oxidative stress. Thus, the data strongly indicate that OBD develops an inflammatory microenvironment even in young mice and amplifies with aging. This study highlights that diet and age are critical factors and have differential impact with age and highlights the interorgan communication for immune defense. Although during young age OBD resolved inflammation irrespective with limited dysbiosis, in contrast, in aging, the same OBD triggered nonresolving inflammation, which is multifactorial in acute HF (Fig. 8*D*). Thus, the current study investigated how aging-OBD dysregulated interaction with microbiome in acute HF. Future preclinical and clinical studies are warranted of chronic HF that will delineate how immune response is regulated in obesity and aging.

CONCLUSIONS

An OBD superimposed onto aging has a critical interaction with gut microbial flora that may misfeed the immune system. An enrichment or imbalance of fatty acids in aging expanded actinobacteria phylum, altered inter-organ coordination, increased proinflammatory mediators, and miscalibrated leukocyte profiling with neutrophil swarming and splenic remodeling, thereby showing signs of nonresolving inflammation in cardiac healing. FJ

ACKNOWLEDGMENTS

The authors acknowledge support from U.S. National Institutes of Health (NIH) National Center for Complementary and Integrative Health (NCCIH) (formerly known as

NCCAM) Grants AT006704 and HL132989, a University of Alabama at Birmingham (UAB) Pittman Scholar Award (to G.V.H.), and an American Heart Association postdoctoral fellowship (POST31000008 to V.K.). The authors also acknowledge the support of the Microbiome Resource, Comprehensive Cancer Center (P30AR050948), Center for Clinical Translational Science (UL1TR001417), University-Wide Institutional Core, Heflin Center for Genomic Sciences, and Microbiome Center at the University of Alabama at Birmingham. The authors declare no conflicts of interest.

AUTHOR CONTRIBUTIONS

G. V. Halade designed and executed the research; V. Kain, W. Van Der Pol, N. Mariappan, P. Eipers, C. Gladine, C. Vigor, and G. V. Halade performed research; V. Kain, A. Ahmad, D. L. Gibson, T. Durand, C. Morrow, and G. V. Halade contributed to analytical tools and analyses of data; and V. Kain, C. Morrow, and G. V. Halade wrote the manuscript with analytical input from other coauthors.

REFERENCES

1. Mozaffarian, D. (2016) Dietary and policy priorities for cardiovascular disease, diabetes, and obesity: a comprehensive review. *Circulation* **133**, 187–225
2. Vigen, R., Maddox, T. M., and Allen, L. A. (2012) Aging of the United States population: impact on heart failure. *Curr. Heart Fail. Rep.* **9**, 369–374
3. Lopez, E. F., Kabarowski, J. H., Ingle, K. A., Kain, V., Barnes, S., Crossman, D. K., Lindsey, M. L., and Halade, G. V. (2015) Obesity superimposed on aging magnifies inflammation and delays the resolving response after myocardial infarction. *Am. J. Physiol. Heart Circ. Physiol.* **308**, H269–H280
4. Halade, G. V., and Kain, V. (2017) Obesity and cardiometabolic defects in heart failure pathology. *Compr. Physiol.* **7**, 1463–1477
5. Willett, W. C. (2007) The role of dietary n-6 fatty acids in the prevention of cardiovascular disease. *J. Cardiovasc. Med. (Hagerstown)* **8** (Suppl 1), S42–S45
6. Ludwig, D. S., Willett, W. C., Volek, J. S., and Neuhouser, M. L. (2018) Dietary fat: from foe to friend? *Science* **362**, 764–770
7. Belkaid, Y., and Hand, T. W. (2014) Role of the microbiota in immunity and inflammation. *Cell* **157**, 121–141
8. Ley, R. E., Bäckhed, F., Turnbaugh, P., Lozupone, C. A., Knight, R. D., and Gordon, J. I. (2005) Obesity alters gut microbial ecology. *Proc. Natl. Acad. Sci. USA* **102**, 11070–11075
9. Chung, H., Pamp, S. J., Hill, J. A., Surana, N. K., Edelman, S. M., Troy, E. B., Reading, N. C., Villablanca, E. J., Wang, S., Mora, J. R., Umesaki, Y., Mathis, D., Benoist, C., Relman, D. A., and Kasper, D. L. (2012) Gut immune maturation depends on colonization with a host-specific microbiota. *Cell* **149**, 1578–1593
10. Rongvaux, A., Takizawa, H., Strowig, T., Willinger, T., Eynon, E. E., Flavell, R. A., and Manz, M. G. (2013) Human hemato-lymphoid system mice: current use and future potential for medicine. *Annu. Rev. Immunol.* **31**, 635–674
11. Haley, P. J. (2003) Species differences in the structure and function of the immune system. *Toxicology* **188**, 49–71
12. Mestas, J., and Hughes, C. C. (2004) Of mice and not men: differences between mouse and human immunology. *J. Immunol.* **172**, 2731–2738
13. Ghosh, S., Molcan, E., DeCoffe, D., Dai, C., and Gibson, D. L. (2013) Diets rich in n-6 PUFA induce intestinal microbial dysbiosis in aged mice. *Br. J. Nutr.* **110**, 515–523
14. DeGruttola, A. K., Low, D., Mizoguchi, A., and Mizoguchi, E. (2016) Current understanding of dysbiosis in disease in human and animal models. *Inflamm. Bowel Dis.* **22**, 1137–1150
15. Kalupahana, N. S., Claycombe, K. J., and Moustaid-Moussa, N. (2011) (n-3) fatty acids alleviate adipose tissue inflammation and insulin resistance: mechanistic insights. *Adv. Nutr.* **2**, 304–316
16. Ander, B. P., Dupasquier, C. M., Prociuk, M. A., and Pierce, G. N. (2003) Polyunsaturated fatty acids and their effects on cardiovascular disease. *Exp. Clin. Cardiol.* **8**, 164–172
17. Kain, V., Prabhu, S. D., and Halade, G. V. (2014) Inflammation revisited: inflammation versus resolution of inflammation following myocardial infarction. *Basic Res. Cardiol.* **109**, 444
18. Beam, J., Botta, A., Ye, J., Soliman, H., Matier, B. J., Forrest, M., MacLeod, K. M., and Ghosh, S. (2015) Excess linoleic acid increases collagen I/III ratio and "stiffens" the heart muscle following high fat diets. *J. Biol. Chem.* **290**, 23371–23384
19. Wong, C. K., Botta, A., Pither, J., Dai, C., Gibson, W. T., and Ghosh, S. (2015) A high-fat diet rich in corn oil reduces spontaneous locomotor activity and induces insulin resistance in mice. *J. Nutr. Biochem.* **26**, 319–326
20. Ley, R. E., Turnbaugh, P. J., Klein, S., and Gordon, J. I. (2006) Microbial ecology: human gut microbes associated with obesity. *Nature* **444**, 1022–1023
21. Mariat, D., Firmesse, O., Levenez, F., Guimarães, V., Sokol, H., Doré, J., Corthier, G., and Furet, J. P. (2009) The Firmicutes/Bacteroidetes ratio of the human microbiota changes with age. *BMC Microbiol.* **9**, 123
22. Turnbaugh, P. J., Ley, R. E., Mahowald, M. A., Magrini, V., Mardis, E. R., and Gordon, J. I. (2006) An obesity-associated gut microbiome with increased capacity for energy harvest. *Nature* **444**, 1027–1031
23. Kumar, R., Eipers, P., Little, R. B., Crowley, M., Crossman, D. K., Lefkowitz, E. J., and Morrow, C. D. (2014) Getting started with microbiome analysis: sample acquisition to bioinformatics. *Curr. Protoc. Hum. Genet.* **82**, 18.8.1–18.8.29
24. Caporaso, J. G., Lauber, C. L., Walters, W. A., Berg-Lyons, D., Lozupone, C. A., Turnbaugh, P. J., Fierer, N., and Knight, R. (2011) Global patterns of 16S rRNA diversity at a depth of millions of sequences per sample. *Proc. Natl. Acad. Sci. USA* **108** (Suppl 1), 4516–4522
25. Liu, Z., Lozupone, C., Hamady, M., Bushman, F. D., and Knight, R. (2007) Short pyrosequencing reads suffice for accurate microbial community analysis. *Nucleic Acids Res.* **35**, e120
26. Caporaso, J. G., Kuczynski, J., Stombaugh, J., Bittinger, K., Bushman, F. D., Costello, E. K., Fierer, N., Peña, A. G., Goodrich, J. K., Gordon, J. I., Huttley, G. A., Kelley, S. T., Knights, D., Koenig, J. E., Ley, R. E., Lozupone, C. A., McDonald, D., Muegge, B. D., Pirrung, M., Reeder, J., Sevinsky, J. R., Turnbaugh, P. J., Walters, W. A., Widmann, J., Yatsunenko, T., Zaneveld, J., and Knight, R. (2010) QIIME allows analysis of high-throughput community sequencing data. *Nat. Methods* **7**, 335–336
27. Halade, G. V., Kain, V., Black, L. M., Prabhu, S. D., and Ingle, K. A. (2016) Aging dysregulates D- and E-series resolvins to modulate cardiosplenic and cardiorenal network following myocardial infarction. *Aging (Albany N.Y.)* **8**, 2611–2634
28. Halade, G. V., Kain, V., and Ingle, K. A. (2018) Heart functional and structural compendium of cardiosplenic and cardiorenal networks in acute and chronic heart failure pathology. *Am. J. Physiol. Heart Circ. Physiol.* **314**, H255–H267
29. Kain, V., Ingle, K. A., Kabarowski, J., Barnes, S., Limdi, N. A., Prabhu, S. D., and Halade, G. V. (2018) Genetic deletion of 12/15 lipoxygenase promotes effective resolution of inflammation following myocardial infarction. *J. Mol. Cell. Cardiol.* **118**, 70–80
30. Galano, J. M., Lee, Y. Y., Oger, C., Vigor, C., Vercauteren, J., Durand, T., Giera, M., and Lee, J. C. (2017) Isoprostanes, neuroprostanes and phytoprostanes: an overview of 25years of research in chemistry and biology. *Prog. Lipid Res.* **68**, 83–108
31. Leung, K. S., Chen, X., Zhong, W., Yu, A. C., and Lee, C. Y. (2014) Microbubble-mediated sonoporation amplified lipid peroxidation of Jurkat cells. *Chem. Phys. Lipids* **180**, 53–60
32. Yonny, M. E., Rodríguez Torresi, A., Cuyamendous, C., Réversat, G., Oger, C., Galano, J. M., Durand, T., Vigor, C., and Nazareno, M. A. (2016) Thermal stress in melon plants: phytoprostanes and phytofurans as oxidative stress biomarkers and the effect of antioxidant supplementation. *J. Agric. Food Chem.* **64**, 8296–8304
33. Ormerod, K. L., Wood, D. L., Lachner, N., Gellatly, S. L., Daly, J. N., Parsons, J. D., Dal'Molin, C. G., Palfreyman, R. W., Nielsen, L. K., Cooper, M. A., Morrison, M., Hansbro, P. M., and Hugenholtz, P. (2016) Genomic characterization of the uncultured Bacteroidales family S24-7 inhabiting the guts of homeothermic animals. *Microbiome* **4**, 36
34. Chang, D. H., Rhee, M. S., Ahn, S., Bang, B. H., Oh, J. E., Lee, H. K., and Kim, B. C. (2015) Faecalibaculum rodentium gen. nov., sp. nov., isolated from the faeces of a laboratory mouse. *Antonie van Leeuwenhoek* **108**, 1309–1318; erratum: 109, 481
35. Halade, G. V., Norris, P. C., Kain, V., Serhan, C. N., and Ingle, K. A. (2018) Splenic leukocytes define the resolution of inflammation in heart failure. *Sci. Signal.* **11**, eaao1818

36. Gupta, P., Lai, S. M., Sheng, J., Tetlak, P., Balachander, A., Claser, C., Renia, L., Karjalainen, K., and Ruedl, C. (2016) Tissue-resident CD169(+) macrophages form a crucial front line against plasmodium infection. *Cell Rep.* **16**, 1749–1761
37. Perez, O. A., Yeung, S. T., Vera-Licona, P., Romagnoli, P. A., Samji, T., Ural, B. B., Maher, L., Tanaka, M., and Khanna, K. M. (2017) CD169^{+} macrophages orchestrate innate immune responses by regulating bacterial localization in the spleen. *Sci. Immunol.* **2**, eaah5520
38. Sacks, F. M., Lichtenstein, A. H., Wu, J. H. Y., Appel, L. J., Creager, M. A., Kris-Etherton, P. M., Miller, M., Rimm, E. B., Rudel, L. L., Robinson, J. G., Stone, N. J., and Van Horn, L. V.; American Heart Association. (2017) Dietary fats and cardiovascular disease: a presidential advisory from the American Heart Association. *Circulation* **136**, e1–e23; erratum: e195
39. Kain, V., Ingle, K. A., Kachman, M., Baum, H., Shanmugam, G., Rajasekaran, N. S., Young, M. E., and Halade, G. V. (2018) Excess ω-6 fatty acids influx in aging drives metabolic dysregulation, electrocardiographic alterations, and low-grade chronic inflammation. *Am. J. Physiol. Heart Circ. Physiol.* **314**, H160–H169
40. Kitai, T., Kirsop, J., and Tang, W. H. (2016) Exploring the microbiome in heart failure. *Curr. Heart Fail. Rep.* **13**, 103–109
41. Arora, T., Anastasovska, J., Gibson, G., Tuohy, K., Sharma, R. K., Bell, J., and Frost, G. (2012) Effect of Lactobacillus acidophilus NCDC 13 supplementation on the progression of obesity in diet-induced obese mice. *Br. J. Nutr.* **108**, 1382–1389
42. Tang, W. H., Wang, Z., Levison, B. S., Koeth, R. A., Britt, E. B., Fu, X., Wu, Y., and Hazen, S. L. (2013) Intestinal microbial metabolism of phosphatidylcholine and cardiovascular risk. *N. Engl. J. Med.* **368**, 1575–1584
43. O'Toole, P. W., and Jeffery, I. B. (2015) Gut microbiota and aging. *Science* **350**, 1214–1215
44. Biagi, E., Nylund, L., Candela, M., Ostan, R., Bucci, L., Pini, E., Nikkïla, J., Monti, D., Satokari, R., Franceschi, C., Brigidi, P., and De Vos, W. (2010) Through ageing, and beyond: gut microbiota and inflammatory status in seniors and centenarians. *PLoS One* **5**, e10667; erratum, 10.1371/annotation/df45912f-d15c-44ab-8312-e7ec0607604d
45. Boulangé, C. L., Neves, A. L., Chilloux, J., Nicholson, J. K., and Dumas, M. E. (2016) Impact of the gut microbiota on inflammation, obesity, and metabolic disease. *Genome Med.* **8**, 42
46. Gill, H. S., Rutherfurd, K. J., and Cross, M. L. (2001) Dietary probiotic supplementation enhances natural killer cell activity in the elderly: an investigation of age-related immunological changes. *J. Clin. Immunol.* **21**, 264–271
47. Gill, H. S., Rutherfurd, K. J., Cross, M. L., and Gopal, P. K. (2001) Enhancement of immunity in the elderly by dietary supplementation with the probiotic Bifidobacterium lactis HN019. *Am. J. Clin. Nutr.* **74**, 833–839
48. Bronte, V., and Pittet, M. J. (2013) The spleen in local and systemic regulation of immunity. *Immunity* **39**, 806–818
49. Jadapalli, J. K., Wright, G. W., Kain, V., Sherwani, M. A., Sonkar, R., Yusuf, N., and Halade, G. V. (2018) Doxorubicin triggers splenic contraction and irreversible dysregulation of COX and LOX that alters the inflammation-resolution program in the myocardium. *Am. J. Physiol. Heart Circ. Physiol.* **315**, H1091–H1100
50. Ponnappan, S., and Ponnappan, U. (2011) Aging and immune function: molecular mechanisms to interventions. *Antioxid. Redox Signal.* **14**, 1551–1585
51. Halade, G. V., Kain, V., Wright, G. M., and Jadapalli, J. K. (2018) Subacute treatment of carprofen facilitate splenocardiac resolution deficit in cardiac injury. *J. Leukoc. Biol.* **104**, 1173–1186
52. Mehta, J., Dinerman, J., Mehta, P., Saldeen, T. G., Lawson, D., Donnelly, W. H., and Wallin, R. (1989) Neutrophil function in ischemic heart disease. *Circulation* **79**, 549–556
53. Haumer, M., Amighi, J., Exner, M., Mlekusch, W., Sabeti, S., Schlager, O., Schwarzinger, I., Wagner, O., Minar, E., and Schillinger, M. (2005) Association of neutrophils and future cardiovascular events in patients with peripheral artery disease. *J. Vasc. Surg.* **41**, 610–617
54. Bauer, J., Ripperger, A., Frantz, S., Ergün, S., Schwedhelm, E., and Benndorf, R. A. (2014) Pathophysiology of isoprostanes in the cardiovascular system: implications of isoprostane-mediated thromboxane A2 receptor activation. *Br. J. Pharmacol.* **171**, 3115–3131
55. Basu, S. (2010) Bioactive eicosanoids: role of prostaglandin F(2α) and F_2-isoprostanes in inflammation and oxidative stress related pathology. *Mol. Cells* **30**, 383–391